DOI: 10.17725/rensit.2023.15.193

# Calculation of rolling stock movement along the railway track by the grid-characteristic method

**[1,2]Anton A. Kozhemyachenko**

[1]Moscow Institute of Physics and Technology, https://mipt.ru/
Dolgoprudny 141700, Moscow region, Russian Federation
[2]Scientific Research Institute of System Analysis of RAS, https://www.niisi.ru/
Moscow 117218, Russian Federation
*E-mail: anton-kozhemyachenko@yandex.ru*

*Received May 04, 2023, peer-reviewed May 11, 2023, accepted May 18, 2023*

*Abstract:* **The application of a grid-characteristic method is proposed for numerical simulation of the movement of rolling stock along a railway track laid on an earth and a bridge. In the study, the railway track is presented using a dynamic system of equations of the theory of elasticity of hyperbolic type. The grid-characteristic method relies on the characteristic properties of the system under consideration and uses finite-difference schemes of high order of accuracy to obtain a space-time solution. The features of railway structures are considered by changing the boundary conditions and conditions at the contact borders. To simulate the areas of contact of wheel pairs of rolling stock with the rail – the "wheel-rail" system – a previously developed pressure boundary condition is applied, modified so as to consider multi-element rolling stock. As a result of computer simulation of the movement of rolling stock along the railway track of various types, full-wave stress distribution in the track structure is obtained, which makes it possible to predict dangerous sections of rolling stock movement.**

*Keywords:* **computer simulation, grid-characteristic method, wheel-rail, rolling stock, railway track**

**UDC 519.63**

*Acknowledgements:* The work was carried out within the framework of the state task of the Federal State Institution «Scientific Research Institute for System Analysis of the Russian Academy of Sciences» on the topic No. FNEF-2022-0005 "Mathematical Modeling of Dynamic Processes in Deformable and Reacting Media using Multiprocessor Computing Systems", Reg. No. 1021060708369-1-1.2.1.

*For citation:* Anton A. Kozhemyachenko. Calculation of the movement of rolling stock along the railway track by the grid-characteristic method. *RENSIT: Radioelectronics. Nanosystems. Information Technologies,* 2023, 15(2):193-198e. DOI: 10.17725/rensit.2023.15.193.

**Contents**



## 1. INTRODUCTION

The problems of monitoring and safety during railway transportation have significant importance for the development of heavy-weight and high-speed movement of rolling stock in various operating conditions. Much attention is paid to the problems of force modeling in the "wheel-rail" system, the analysis of contact spots and wear models of wheel sets and rails [1-5], the design features of the track [6-7], movement on ballast and with riding on slabs of the railway track [8-10].

For numerical modeling of this class of problems finite element approaches, Galerkin

methods [11-15] are often used, including commercial software ANSYS, ABAQUS, etc.

In this paper, we propose the application of the grid-characteristic method that allows us to consider the problems of rolling stock movement in a dynamic formulation and to investigate the influence of wave processes during rolling stock movement using finite-difference schemes of high order accuracy in time and space [16-18].

## 2. MODELS AND METHODS

For numerical simulation of the problem of train movement, the railway track is represented as a set of layers of an isotropic linear elastic medium described in the two-dimensional case by a system of equations:

$$\frac{\partial \mathbf{q}}{\partial t} + \mathbf{A}_1 \frac{\partial \mathbf{q}}{\partial x} + \mathbf{A}_2 \frac{\partial \mathbf{q}}{\partial y} = 0, \quad (1)$$

$$\mathbf{q} = (v_x, v_y, \sigma_{xx}, \sigma_{yy}, \sigma_{xy})^T, \quad (2)$$

$$\mathbf{A}_1 = \begin{pmatrix} 0 & 0 & -\frac{1}{\rho} & 0 & 0 \\ 0 & 0 & 0 & 0 & -\frac{1}{\rho} \\ -\lambda-2\mu & 0 & 0 & 0 & 0 \\ -\lambda & 0 & 0 & 0 & 0 \\ 0 & -\mu & 0 & 0 & 0 \end{pmatrix},$$

$$\mathbf{A}_2 = \begin{pmatrix} 0 & 0 & 0 & 0 & -\frac{1}{\rho} \\ 0 & 0 & 0 & -\frac{1}{\rho} & 0 \\ 0 & -\lambda & 0 & 0 & 0 \\ 0 & -\lambda-2\mu & 0 & 0 & 0 \\ -\mu & 0 & 0 & 0 & 0 \end{pmatrix}, \quad (3)$$

where in (2) $\mathbf{q}$ – the vector of the initial functions, which include the components of the perturbation propagation velocity $\mathbf{v}$ and the components of the symmetric Cauchy stress tensor $\boldsymbol{\sigma}$, in (3) $\lambda$, $\mu$ – the Lame parameters that determine the elastic properties of the material. Matrices $\mathbf{A}_1$, $\mathbf{A}_2$ have a set of eigenvalues $\{c_P, -c_P, c_S, -c_S, 0\}$, where $c_P = \sqrt{(\lambda+2\mu)/\rho}$ – velocity of propagation of longitudinal waves, $c_S = \sqrt{\mu/\rho}$ – velocity of propagation of transverse waves. Thus, initial system (1) is hyperbolic, which means that the matrices $\mathbf{A}_1$, $\mathbf{A}_2$ can be represented as

$$\mathbf{A} = \boldsymbol{\Omega}\boldsymbol{\Lambda}\boldsymbol{\Omega}^{-1},$$

where the matrix $\boldsymbol{\Omega}$ consists of columns that are the right eigenvectors of the original matrix, which, in turn, correspond to the eigenvalues, which are elements of the diagonal matrix $\boldsymbol{\Lambda}$. Splitting the system (1) in spatial directions and using the transition to Riemann invariants $\boldsymbol{\omega} = \boldsymbol{\Omega}^{-1}\mathbf{q}$, which are transferred according to the characteristics of the hyperbolic system, we obtain the hyperbolic system from linear transfer equations with constant coefficients in Riemann invariants

$$\frac{\partial \boldsymbol{\omega}}{\partial t} + \boldsymbol{\Lambda}\frac{\partial \boldsymbol{\omega}}{\partial x} = 0. \quad (4)$$

The system in Riemann invariants (4) on the upper layer in time can be numerically integrated using finite-difference schemes, for example, using the Rusanov scheme [19], used in calculations in this paper, of the third order in time and space. To move to the components $\mathbf{v}$ and $\boldsymbol{\sigma}$ on the upper layer in time after calculating the Riemann invariants, the inverse transformation is used $\mathbf{q} = \boldsymbol{\Omega}\boldsymbol{\omega}$.

The basic model of the construction of a railway track laid on the earthen bed is shown in **Fig. 1**, and on the bridge structure in **Fig. 2**. The

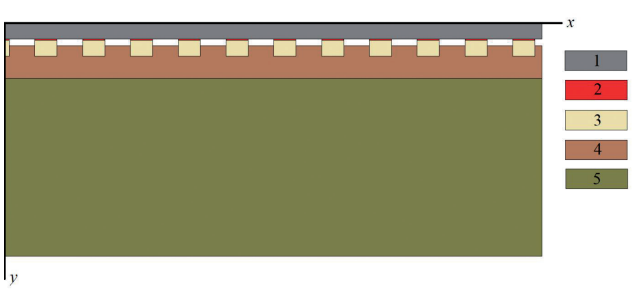


**Fig. 1**. *The railway track laid on the roadbed: 1 – rail, 2 – dampers, 3 – sleepers, 4 – ballast, 5 – earthen bed.*

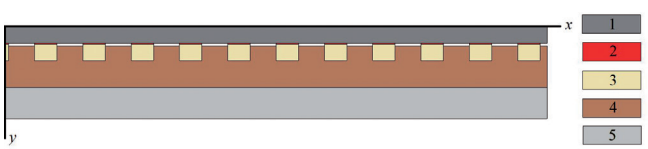


**Fig. 2.** *Railway track on the bridge: 1 – rail, 2 – dampers, 3 – sleepers, 4 – ballast, 5 – supporting structure.*

**Table 1**

Elastic parameters of media.

| Medium | Velocity P-waves, m/s | Velocity S-waves, m/s | Density, kg/m³ |
|---|---|---|---|
| Rail | 5740 | 3092 | 7800 |
| Damper | 700 | 120 | 1200 |
| Sleeper | 4200 | 2200 | 2500 |
| Balast | 500 | 300 | 1400 |
| Earthen bed | 2000 | 1000 | 2000 |
| Supporting structure | 4200 | 2200 | 2500 |

elastic characteristics of the media are given in **Table 1**. The total length of the track section in both cases was 25 m. Free boundary conditions were set at the boundaries of the media that were elements of the corresponding model

$$\boldsymbol{\sigma}\cdot\mathbf{n} = 0, \quad (5)$$

where $\mathbf{n}$ – normal to the corresponding boundary.

Between the contact media (medium 1 and medium 2), a condition of complete adhesion is set at the contact boundary, which is described by the expressions

$$\mathbf{v}_1 = \mathbf{v}_2,$$

$$\boldsymbol{\sigma}_1\cdot\mathbf{n} = \boldsymbol{\sigma}_2\cdot\mathbf{n},$$

here $\mathbf{n}$ – normal to the boundary of the contacting medium 1.

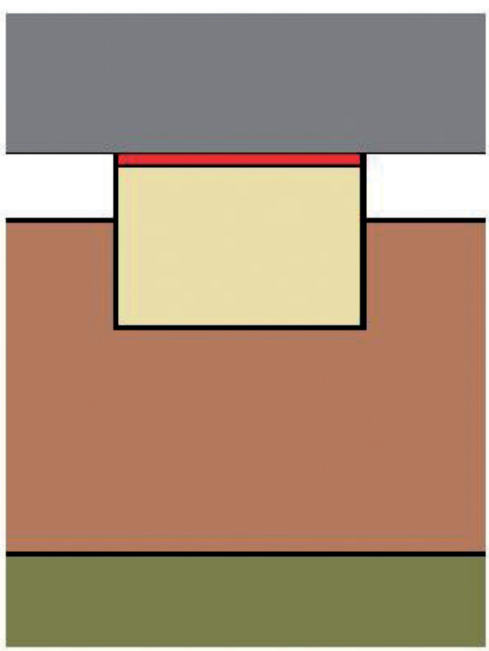

**Fig. 3.** *The position of the damper (red) between the rail and the sleeper.*

Absorption conditions are used on the left and right boundaries of the integration regions in Fig. 1 and Fig. 2. Similarly, this condition is used for the lower boundary of the integration region in Fig. 1 for the sedimentary rock layer. In the case of a bridge structure, a free boundary condition is set at the lower boundary of the supporting structure (5). Between the rail and the sleeper, a damper is used in both settings for clarity, shown separately in **Fig. 3**.

To simulate the movement of rolling stock along the railway track from Fig. 1 and Fig. 2, the force boundary condition in the wheel-rail system from [16] is used with the modification that allows to consider several elements of the rolling stock at once in **Fig. 4**. The geometric parameters of the rolling stock element are $H_{TRAIN}$ = 7.7 m, $L_{TRAIN}$ = 1.85 m, mass 90 t. The pressure of the wheel without defects on the rail in the "wheel-rail" system is equal 188 MPa.

In the calculation the integration areas in Fig. 1 and Fig. 2 were covered with rectangular calculation meshes with the constant step for the corresponding medium according to **Table 2**, the integration step in time was $10^{-7}$ s.

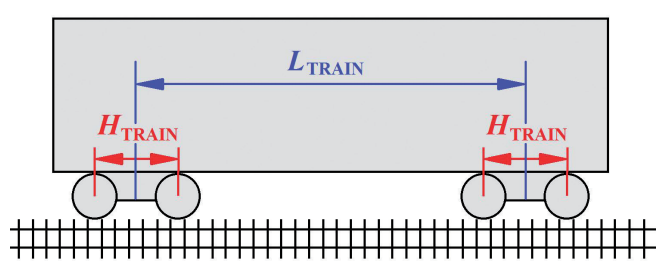


**Fig. 4.** *Rolling stock element.*

**Table 2**

Meshes parameters.

| Medium | Step along OX, m | Step along OY, m |
|---|---|---|
| Rail | 0.01 | 0.005 |
| Damper | 0.01 | 0.001 |
| Sleeper | 0.01 | 0.005 |
| Balast | 0.01 | 0.005 |
| Earthen bed | 0.01 | 0.010 |
| Supporting structure | 0.01 | 0.010 |

## 3. RESULTS AND DISCUSSION

**Fig. 5** and **Fig. 6** show the results of calculations of the dynamic load distribution of the vertical component of the Cauchy stress tensor at various points in time when the rolling stock consisting of two elements is moving along the railway track laid on the earthen bed with the velocity of 120 km/h and on a bridge with the velocity of 72 km/h, respectively. To account for the slow increase in stresses due to the interaction of the train and the rail from zero to a set value in the wheel-rail system 170000 iterations have performed. The total number of iterations over time is 680000, i.e. the total movement time of the rolling stock is 0.051 s.

The obtained results show the importance of consideration in the mathematical model the number of relevant standards of railway

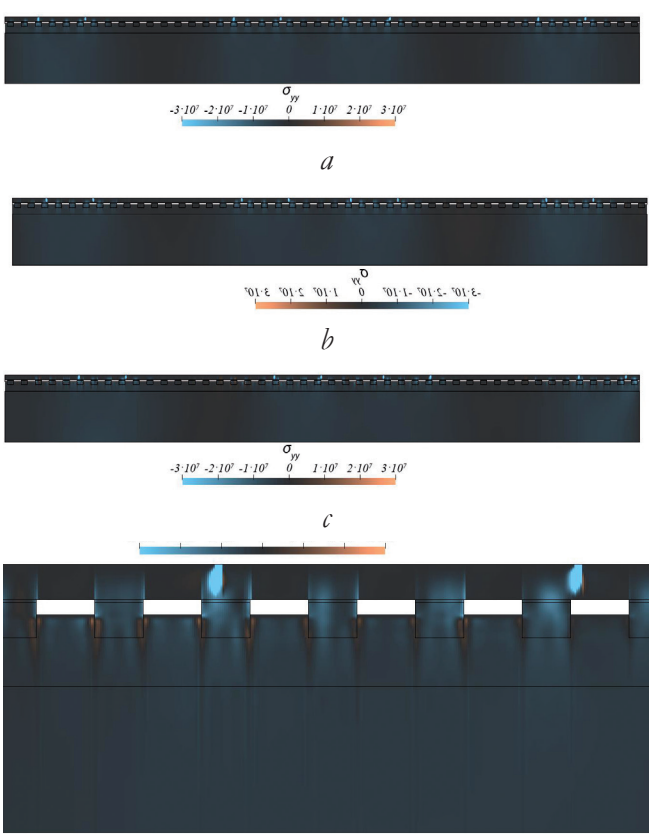

*a*

*b*

*c*

*d*

**Рис. 5**. *The movement of the rolling stock of two elements on the earthen bed: a – the beginning of movement, b – 0.0255 s, c – 0.051 s, d – the enlarged picture on the left at 0.051 s.*

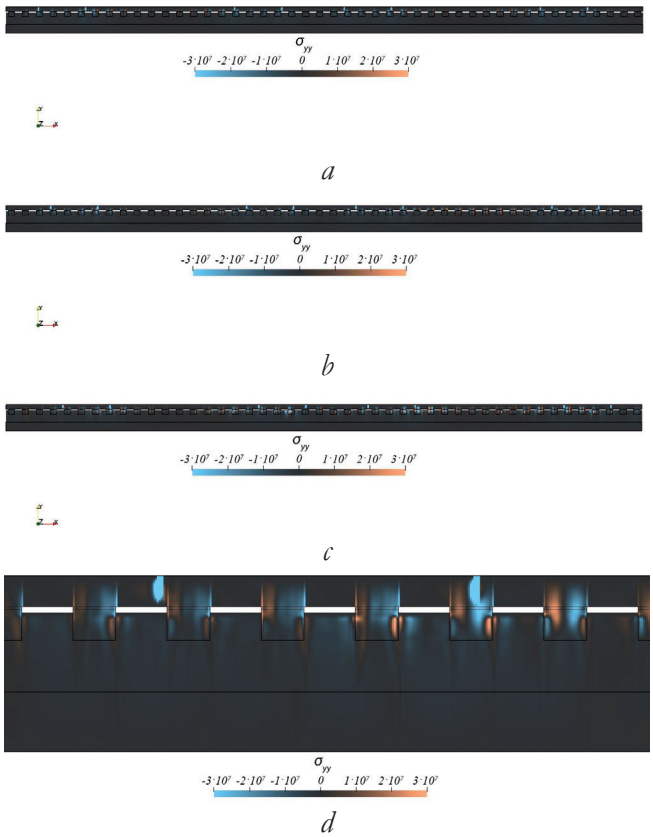

*a*

*b*

*c*

*d*

**Рис. 6**. *The movement of the rolling stock of two elements on the bridge: a – the beginning of movement, b – 0.0255 s, c – 0.051 s, d – the enlarged picture on the left at 0.051 s.*

track design, some of which were not consider earlier in [16-18]: the presence of the damping layer between rails and sleepers, the use of reinforced concrete sleepers, unlike wooden ones. Due to the modification of the boundary condition used, it is possible to specify the rolling stock consisting of a large number of elements. When comparing the wave patterns in Fig. 4 and Fig. 5 it can be seen that when moving on the bridge, the more pronounced stress pattern is formed in the bridge structure in the area of the rail-damper-sleeper junction than when moving along the earthen bed. This is due to the fact that in the case of movement along the earthen bed, the wave front propagate into the thickness of sedimentary rocks, whereas on the lower surface of the bridge, the incoming wave front is reflected back into the track structure.

## 4. CONCLUSIONS

Using the grid-characteristic method on structured rectangular meshes in combination with the modification of the boundary condition for the wheel-rail system, it is possible to obtain stress distributions during the movement of rolling stock consisting of the large number of elements along the railway track at various points in time. The proposed approach and mathematical models make it possible to consider the damping layer between rails and sleepers, change the parameters and type of construction using various types of contact and boundary conditions, speed mode. The obtained algorithms and models can be used to analyze wave effects during the movement of rolling stock and to formulate the problem of the movement of rolling stock in conditions of transition from the railway track laid on an earthen bed to the track laid in conditions of the bridge structure, considering changes in the rigidity of the sub-rail base.

## REFERENCES

1. Six K, Mihalj T, Trummer G, Marte C, Krishna VV, Nia SH, Stichel S. Assesment of running gear performance in relation to rolling contact fatigue of wheels and rails based on stochastic simulations. *Proceedings of the Institution of Mechanical Engineers Part F Journal of Rail and Rapid Transit,* 2019, 234(4):0954409719879600. DOI: 10.1177/0954409719879600.
2. Goryacheva I, Torskaya EV. Modeling the Accumulation of Contact Fatigue Damage in Materials with Residual Stresses under Rolling Friction. *Journal of Friction and Wear*, 2019, 40(1):33-38.
3. Torskaya EV, Goryacheva IG, Muravyeva TI, Shcerbakova OO, Tsukanov IY, Meshcheryakova AR, Shkaley IV, Zagranichek KL, Zakharov SM, Shur EA. Rolling Contact Fatigue Damage in Welded Rail Steel Joints. *Physical Mesomechanics,* 2023, 26(1):7-18; doi: 10.1134/S1029959923010022.
4. Loktev AA, Korolev VV, Shishkina IV, Basovsky DA. Modeling the Dynamic Behavior of the Upper Structure of the Railway Track. *Procedia Engineering*, 2017, 189:133-137. DOI: 10.1016/j.proeng.2017.05.022.
5. Huang YB, Shi LB, Zhao XJ, Cai ZB, Liu QY, Wang WJ. On the formation and damage mechanism of rolling contact fatigue surface cracks of wheel/rail under dry condition. Wear, 2018, 400:62-73. DOI: 10.1016/j.wear.2017.12.020.
6. Zakeri JA, Rezvani FH. Failures of railway concrete sleepers during service life. International *Journal of Construction Engineering and Management*, 2012, 1(1):1-5.
7. Ngamkhanong C, Kaewunruen S, Costa BJA. State-of-the-art review of railway track resilience monitoring. *Infrastructures*, 2018, 3(1):3.
8. Liu K, Lombaert G, De Roeck G. Dynamic analysis of multi-span viaducts under the passage of the train using a substructure approach. *Bridge Engineering,* 2014, 19(1):83-90.
9. Poliakov V, Dang TN. Wheel-rail impact interaction on the high-speed railroad bridges. *Russian Journal of Transort Engineering,* 2019, 6(1):15SATS119.
10. Charoenwong C, Connolly DP, Colaco A, Alves Costa P, Woodward PK, Romero A, Galvin P. Railway slab vs ballasted track: A comparison of track geometry degradation. *Construction and Building Materials*, 378:131121.
11. Adak D, Pramod A, Ooi E, Natarajan S. A comined virtual element method and the scaled boundary finite element method for linear elastic fracture mechanics. *Eng. Anal. Boundary Elem*, 2020, 113:9-16.
12. Tang Z, Liu F, Guo S, Chang J, Zhang J. Evaluation coupled finite element/meshfree method for a robust full-scale crashworthiness simulation of railway vechicles. *Adv. Mech. Eng,* 2016, 8:1687814016642954.

13. Nejad R, Liu Z, Ma W, Berto F. Reliability analysis of fatigue crack growth for rail steel under variable amplitude service loading conditions and wear. *Int. J. Fatigue*, 2021, 152:106450.
14. Krishnamoorthy RR, Saleheen Z, Effendy A, Alisibramulisi A, Awaludin A. The Effect of Rubber Pads on The Stress Distribution for Concrete Railway Sleepers. *IOP Conference Series Materials Science and Engineering*, 2018, 431(11):112007.
15. Shahraki M, Warnakulasooriya C, Witt KJ. Numerical Study of Transition Zone Between Ballasted and Ballastless Railway Track. *Transportation Geotechnics*, 2015, 3:58-67.
16. Kozhemyachenko AA, Petrov IB, Favorskaya AV, Khokhlov NI. Boundary conditions for modeling the impact of wheels on railway track. *Comput. Math. Math. Phys.*, 2020, 60(9):1539-1554.
17. Kozhemyachenko AA, Petrov IB, Favorskaya AV. Calculation of the stress state of a railway track with unsupported sleepers using the grid-characteristic method. *J. Appl. Mech. Tech. Phys.,* 2021, 62:344-350.
18. Koyhemzachenko AA, Kabanova AS, Petrov IB, Favorskaya AV. Modeling Movement of Train Along Bridge by Grid-Characteristic Method. Smart Modelling For Engineering Systems. *Smart innovation, Systems and Technologies,* 2021, 214:165-174.
19. Favorskaya A, Khokhlov N. Accounting for curved boundaries in rocks by using curvilinear and Chimera grids. *Procedia Computer Science,* 2021, 192:3787-3794.